APSIPA Transactions on Signal and Information Processing, 2024, 13, e32

Original Paper

Properties of Type-2 Complex Conjugate Pair Sums and Their Applications

Shaik Basheeruddin Shah[1*], Vijay Kumar Chakka[2], Arikatla Satyanarayana Reddy[3], Goli Srikanth[2], Nazar T. Ali[1], Ahmed Altunaiji[1], Mohamed Alhajri[4], Dragan Olcan[5] and Raed Abd-Alhameed[6]

[1]*Department of Electrical Engineering, Khalifa University, Abu Dhabi, UAE*
[2]*Department of Electrical Engineering, Shiv Nadar University, Uttar Pradesh, India*
[3]*Department of Mathematics, Shiv Nadar University, Uttar Pradesh, India*
[4]*Department of Computer Science and Engineering, American University of Sharjah, Sharjah, UAE*
[5]*School of Electrical Engineering, University of Belgrade, Serbia*
[6]*Department of Electronic and Electrical Engineering, University of Bradford, UK*

ABSTRACT

Ramanujan Sum (RS) has recently been used in the Ramanujan Periodic Transform (RPT), which efficiently extracts period information with lower computational complexity. Building on RS and RPT, Complex Conjugate Pair Sums of type-1 (CCPS$^{(1)}$) and type-2 (CCPS$^{(2)}$) have been developed, forming the basis of the Orthogonal Complex Conjugate Periodic Transform (OCCPT), an alternative to the Discrete Fourier Transform (DFT) with reduced computational requirements. While RSs and CCPS$^{(1)}$ properties are well-studied, CCPS$^{(2)}$ characteristics remain underexplored.

*Corresponding author: shaik.shah@ku.ac.ae. This paper is based upon work supported by the Khalifa University of Science and Technology under the KU-Belgrade Joint Research Collaboration.

Received 10 August 2024; revised 11 October 2024; accepted 03 November 2024
ISSN 2048-7703; DOI 10.1561/116.20240056

This paper investigates CCPS$^{(2)}$ properties and their potential applications. Specifically, it examines the behavior of a Linear Time-Invariant (LTI) system with a CCPS$^{(2)}$-based impulse response, demonstrating that the system can approximate first- and second-order derivatives of the input signal. This property is applied to image edge detection and Electrocardiogram (ECG) preprocessing, comparing the performance with systems using RS and CCPS$^{(1)}$ impulse responses. Additionally, the paper shows that the DFT coefficients of any two distinct, CCPS$^{(1)}$ or CCPS$^{(2)}$, as well as CCPS$^{(1)}$ and CCPS$^{(2)}$, sequences are non-overlapping, ensuring orthogonality among the subspaces they span. Based on this, we propose a new modulation scheme, Orthogonal Complex Conjugate Periodic Subspace Division Multiplexing (OCCPSDM), which is compared with existing modulation techniques regarding Peak-to-Average Power Ratio (PAPR) and computational complexity.

Keywords: Complex exponential, Ramanujan sums, complex conjugate pair sums, RPT, OCCPT

1 Introduction

Complex Exponential Sequences (CESs) are fundamental in the mathematical framework of digital signal processing [16]. The well-known discrete Fourier representation utilizes CESs as the basis for representing finite-length signals, enabling the extraction of frequency and period information from the given signal [16, 40, 41]. Recently, the integer-valued Ramanujan Sum (RS), introduced by the Indian mathematician Srinivasa Ramanujan [21], has been employed in a signal representation method called the Ramanujan Periodic Transform (RPT) [40, 41]. RPT is notable for its ability to extract period information from signals with reduced computational complexity. Consequently, RPT has found applications in various fields [19, 25, 36, 38, 24, 30, 29, 28, 32, 11, 23, 13].

Building on the concepts of RS and RPT, the authors in [31, 26] have introduced two summations, termed Complex Conjugate Pair Sum of type-1 (CCPS$^{(1)}$) and Complex Conjugate Pair Sum of type-2 (CCPS$^{(2)}$). These summations form the foundation of an orthogonal representation known as the Orthogonal Complex Conjugate Periodic Transform (OCCPT) [27]. The OCCPT has been shown to extract the same information—namely, frequency and associated period—as the widely used Discrete Fourier Transform (DFT), but with reduced computational complexity. This advancement has significant

implications for applications that require efficient signal-processing techniques [27].

While extensive research has been conducted on properties of CESs, RSs, and CCPS$^{(1)}$, there remains a notable gap in the study of CCPS$^{(2)}$ properties [25, 18, 40, 41, 26, 35, 43]. This paper aims to address this gap by exploring the CCPS$^{(2)}$ properties and their applications in signal processing. Specifically, motivated by the properties of RS and CCPS$^{(1)}$ stated in [40, 41, 26, 43], this paper discusses the following properties:

1. Consider a Linear Time-Invariant (LTI) system characterized by an input signal $x(n)$, an impulse response $h(n)$, and an output $y(n)$. If $h(n)$ is defined by the one-period data of CCPS$^{(2)}$, then we can demonstrate that $y(n)$ approximates the first-order derivative of $x(n)$. Furthermore, we establish that under certain constraints on CCPS$^{(2)}$, the LTI system can also approximate the second-order derivative of the input signal. As applications, we explore image edge detection and Electrocardiogram (ECG) signal preprocessing for enhanced R-peak delineation. We also compare the results obtained using the one-period data of the CCPS$^{(2)}$ impulse response with those obtained using the one-period data of RS and CCPS$^{(1)}$, as the impulse responses of the system. Through comparisons, we demonstrate that CCPS$^{(1)}$ and CCPS$^{(2)}$ extract the same frequency information with a phase shift, validating the fact that they form a Hilbert Transform (HT) pair. Additionally, compared to RS, we demonstrate that both CCPS$^{(1)}$ and CCPS$^{(2)}$ achieve a fine feature extraction.

2. We demonstrate that the DFT coefficients of any two distinct CCPSs$^{(1)}$ or CCPSs$^{(2)}$, as well as CCPS$^{(1)}$ and CCPS$^{(2)}$, do not overlap. This property ensures orthogonality among the subspaces spanned by these summations. Specifically, a CCPS spans a two-dimensional space called Complex Conjugate Subspace (CCS). Based on this finding, we introduce a new modulation scheme named Orthogonal Complex Conjugate Periodic Subspace Division Multiplexing (OCCPSDM). We then compare OCCPSDM with existing modulation schemes and two other new schemes that belong to the Nested Periodic Matrix (NPM) family, focusing on metrics such as Peak-to-Average Power Ratio (PAPR) and computational complexity. We show that OCCPSDM offers comparable PAPR with reduced computational complexity relative to other existing modulation schemes.

The paper is organized as follows. Section 2 provides a review of the fundamental preliminaries necessary for understanding the subsequent discussions. It includes essential definitions and concepts related to our study. Section 3 explores the derivative property of CCPS$^{(2)}$ and its applications. Section 4 examines the property of non-overlapping DFT coefficients of CCPSs and its

application in wireless communication. Section 5 concludes with a summary of our findings.

In this paper, the following notations are employed. The symbols $\mathbb{N}$, $\mathbb{Z}$, and $\mathbb{R}$ denote the sets of natural numbers, integers, and real numbers, respectively. The notation (a, b) represents the Greatest Common Divisor (GCD) of two integers a and b. The floor function $\lfloor a \rfloor$ denotes the greatest integer less than or equal to a real number a. We use $a \mid b$ to indicate that a divides b, and $a \nmid b$ to signify that a does not divide b. Euler's totient function, denoted as φ, is defined by the formula $\varphi(n) = \#U_n$, where $U_n = \{i \in \mathbb{N} \mid 1 \leq i \leq n, (i, n) = 1\}$, which counts the number of integers up to n that are coprime with n. Furthermore, we define the set $\hat{U}_n$ as $\{i \in \mathbb{N} \mid 1 \leq i \leq \lfloor \frac{n}{2} \rfloor, (i, n) = 1, n > 2\}$, which consists of integers less than or equal to $\frac{n}{2}$ that are coprime to n. The cardinality of $\hat{U}_n$ is given by $\#\hat{U}_n = \frac{\varphi(n)}{2}$. The linear convolution between two sequences $x(n)$ and $h(n)$ is denoted as $x(n) * h(n)$.

2 Preliminaries

2.1 First-Order and Second-Order Derivative Approximation

An LTI system characterized by an impulse response acts as an approximation to the first-order derivative if the system output satisfies the following three properties [43, 10, 9]:

- Equal to zero for a constant input.
- Equal to non-zero at the on-transient of a unit step input.
- Equal to a non-zero constant for a given ramp input.

Notably, both unit step and ramp input signals provide a comprehensive understanding of the LTI system's behavior under both transient and steady-state conditions. Along with the first two properties mentioned above, if the system output is zero for a ramp input, then the system acts as an approximation to the second-order derivative [43].

2.2 Definitions of RS and CCPSs

For a given $q \in \mathbb{N}$ and $k \in [0, q-1]$, the CES is defined as $s_{q,k}(n) = e^{\frac{j2\pi kn}{q}}$, where $n \in \mathbb{Z}$. Various summations, such as RS, CCPS$^{(1)}$, and CCPS$^{(2)}$ have been developed in the literature by taking linear combinations of CESs that satisfy certain periodicity property [21, 31, 27]. For instance, let $q = 8$, then $\{s_{8,1}(n), s_{8,3}(n), s_{8,5}(n), s_{8,7}(n)\}$, are the set of CESs with period exactly

equals 8. Using these sequences, RS, CCPS$^{(1)}$, and CCPS$^{(2)}$ are generated as follows:

$$\text{RS: } c_8(n) = e^{\frac{j2\pi(1)n}{8}} + e^{\frac{j2\pi(3)n}{8}} + e^{\frac{j2\pi(5)n}{8}} + e^{\frac{j2\pi(7)n}{8}}.$$

$$\text{CCPS}^{(1)}\text{: } c^{(1)}_{8,k}(n) = e^{\frac{j2\pi(k)n}{8}} + e^{\frac{j2\pi(8-k)n}{8}},\ k{\in}\hat{U}_8 = \{1,3\}.$$

$$\text{CCPS}^{(2)}\text{: } c^{(2)}_{8,k}(n) = \frac{1}{j}\left[e^{\frac{j2\pi(k)n}{8}} - e^{\frac{j2\pi(8-k)n}{8}}\right],\ k{\in}\hat{U}_8 = \{1,3\}.$$

Generalizing the above example, for a given $q{\in}\mathbb{N}$, leads to the following definitions [21, 31, 27]:

$$\text{RS: } c_q(n) = \sum_{\substack{l=1\\(l,q)=1}}^{q} e^{\frac{j2\pi ln}{q}}, \quad \forall n{\in}\mathbb{Z}.$$

$$\text{CCPS}^{(1)}\text{: } c^{(1)}_{q,k}(n) = \begin{cases} 1, & \text{if } q=1 \\ (-1)^n, & \text{if } q=2 \\ 2\cos\left(\frac{2\pi kn}{q}\right), & \text{if } q>2 \end{cases}, \quad \forall n{\in}\mathbb{Z} \text{ and } k{\in}\hat{U}_q. \tag{1}$$

$$\text{CCPS}^{(2)}\text{: } c^{(2)}_{q,k}(n) = \begin{cases} 1, & \text{if } q=1 \\ (-1)^n, & \text{if } q=2 \\ 2\sin\left(\frac{2\pi kn}{q}\right), & \text{if } q>2 \end{cases}, \quad \forall n{\in}\mathbb{Z} \text{ and } k{\in}\hat{U}_q.$$

From (1), $c^{(2)}_{q,k}(n)$ is a q-periodic sequence for any $k{\in}\hat{U}_q$. Furthermore, it has been demonstrated that a two-dimensional Complex Conjugate Subspace (CCS) [5] can be spanned using CCPS$^{(2)}$ and its circular downshift. The authors of [27] explored several fundamental properties of CCPS$^{(2)}$, including orthogonality, summation, and sum-of-squares. However, there is a gap in the literature, [25, 18, 40, 41, 26, 27, 35, 43], concerning the comparison of CCPS$^{(2)}$ properties with RS and CCPS$^{(1)}$. This paper seeks to fill that gap by examining specific properties of CCPS$^{(2)}$. In particular, we focus on two properties in the following sections: derivative approximation and non-overlapping DFT coefficients.

3 CCPS$^{(2)}$ As Derivative Approximation

In this section, we examine a linear time-invariant (LTI) system with an impulse response based on CCPS$^{(2)}$. We establish constraints to ensure that the system's output closely approximates the first or second derivative of its input. Before delving deeper into the analysis, we derive closed-form expressions for the following summations, which will be utilized in the subsequent analysis:

$$S(q,k)=\sum_{n=0}^{q-1}c_{q,k}^{(2)}(n), T(q,k)=\sum_{n=0}^{q-1}nc_{q,k}^{(2)}(n), \text{ and}$$
$$P(q,k,m)=\sum_{n=0}^{q-1}nc_{q,k}^{(2)}(n-m). \tag{2}$$

It is proved in [27] that

$$S(q,k)=0, \text{ for } q>1 \text{ and } k\in\hat{U}_q. \tag{3}$$

However, $T(q,k)=0$ only when $q=1$. If $q=2$, then $T(q,k)=-1$. If $q>2$, then

$$T(q,k)=\frac{1}{j}\left[\sum_{n=0}^{q-1}ne^{\frac{j2\pi kn}{q}}-\sum_{n=0}^{q-1}ne^{\frac{-j2\pi kn}{q}}\right]. \tag{4}$$

By recalling $\sum_{n=0}^{q-1}ne^{\frac{j2\pi kn}{q}}=\frac{-q}{1-e^{\frac{j2\pi k}{q}}}$ and $(q,k)=1$, equation (4) can be simplified as

$$T(q,k)=\frac{-q\sin\left(\frac{2\pi k}{q}\right)}{1-\cos\left(\frac{2\pi k}{q}\right)}\neq 0, \ q>2. \tag{5}$$

Now, consider the summation $P(q,k,m)=\sum_{n=0}^{q-1}nc_{q,k}^{(2)}(n-m)$, where $q>2$ and $1\leq m\leq q-1$. Observe that the term $P(4b+2,k,b)=P(4b+2,k,3b+1)=0$, $\forall b\in\mathbb{N}$ and $\forall k\in\hat{U}_q$. The following result shows that the converse is also true.

Theorem 1. *If $P(q,k,m)=0$, then $q=4b+2$ and $m\in\{b,3b+1\}$.*

Proof. Simplifying $P(q,k,m)$ similar to that of $T(q,k)$, we obtain

$$P(q,k,m)=\frac{q}{1-\cos(v)}\left[\sin(vm)-\sin(v(m+1))\right], \tag{6}$$

where $v=\frac{2\pi k}{q}$. Thus, $P(q,k,m)=0$ only if

$$\sin(vm)-\sin(v(m+1))=2\cos\left(\frac{\pi k(2m+1)}{q}\right)\sin\left(\frac{-\pi k}{q}\right)=0.$$

As $(k,q)=1$, the term $\sin\left(\frac{-\pi k}{q}\right)\neq 0$, and $\cos\left(\frac{\pi k(2m+1)}{q}\right)$ will be zero if $\frac{\pi k(2m+1)}{q}=(2r+1)\frac{\pi}{2}$, where $r\in\mathbb{Z}$. From this, it follows that q is an even number and $k(2m+1)=q_1(2r+1)$, where $q=2q_1$. Using $(k,q)=(k,q_1)=1$, implies $q_1|(2m+1)$; hence q is of the form $4b+2$ and $m=\frac{\alpha q_1-1}{2}$, where $b\in\mathbb{N}$ and $\alpha\in\mathbb{N}$. Finally, $m=b$ or $m=3b+1$ follows from the fact that $1\leq m\leq 2q_1-1$. □

Figure 1 depicts $\sin(vm)-\sin(v(m+1))$ for different values of q and k. One can validate Theorem 1 from these figures as well.

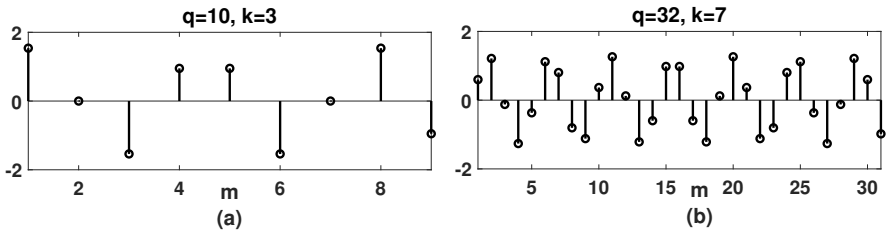

Figure 1: (a)-(b) $\sin(vm) - \sin(v(m+1))$ for different q and k values.

3.1 CCPS$^{(2)}$ as Derivative

Consider an LTI system with impulse response

$$h_q(n) = \hat{c}^{(2)}_{q,k}(n) = \begin{cases} c^{(2)}_{q,k}(n), & 0 \le n \le q-1 \\ 0, & \text{otherwise} \end{cases}, \; q > 1,$$

and analyze the system output, $y(n)$, for different input, $x(n)$, sequences to validate its derivative approximation.

- If $x(n) = C$, where C is a constant value, then

$$y(n) = x(n) * \hat{c}^{(2)}_{q,k}(n) = \sum_{l=0}^{q-1} x(n-l) c^{(2)}_{q,k}(l) = CS(q,k). \tag{7}$$

  Substituting (3) in the above equation leads to $y(n) = 0$.

- If $x(n) = u(n - n_0)$, where $u(n)$ is a unit step sequence, then

$$y(n) = \sum_{l=0}^{q-1} u(n - n_0 - l) c^{(2)}_{q,k}(l). \tag{8}$$

  Again using (3), we can check that $y(n) \neq 0$ for $n_0 < n \le n_0 + q - 2$ (on-transient duration).

- If $x(n) = n$, then

$$y(n) = \sum_{l=0}^{q-1} (n-l) c^{(2)}_{q,k}(l) = nS(q,k) - T(q,k). \tag{9}$$

  Substituting (3) and (5) in the above equation lead to

$$y(n) = \frac{q \sin\left(\frac{2\pi k}{q}\right)}{1 - \cos\left(\frac{2\pi k}{q}\right)}, \; q > 2 \text{ and } k \in \hat{U}_q. \tag{10}$$

The right-hand side term in (10) is independent of the variable n. Moreover, if $q = 2$, then $y(n) = 1$. Hence, for a given ramp input, the system output is equal to a non-zero constant value.

From Section 2.1, we can summarize the above analysis as the following theorem:

Theorem 2. *The linear convolution between the given finite-length signal $x(n)$ and $h_q(n) = \hat{c}^{(2)}_{q,k}(n),\ q > 1$, is an approximation to the first-order derivative of $x(n)$.*

In [43] and [26], it is proved that the linear convolution of $x(n)$ with $\hat{c}_q(n)$ (one period of RS) and $x(n)$ with $\hat{c}^{(1)}_{q,k}(n)$ (one period of CCPS$^{(1)}$) are equivalent to the first-order derivative of $x(n)$, respectively. Further, this operation is also equivalent to the second-order derivative if we consider an odd number q and a circular shift of $\frac{q-1}{2}$ for both $\hat{c}_q(n)$ and $\hat{c}^{(1)}_{q,k}(n)$. This raises the following question: Can a system with $h(n) = \hat{c}^{(2)}_{q,k}(n)$ act as an approximation to the second-order derivative? Since $T(q,k)\neq 0$ in (9), we consider $h_q(n) = \hat{c}^{(2)}_{q,k}(n-m)$, $1 \leq m \leq q-1$. Hence, we replace the term $T(q,k)$ in (9) with $P(q,k,m)$; then the following result is a direct consequence of Theorem 1.

Theorem 3. *If q be of the form $4b+2$ and $m \in \{b, 3b+1\}$, then the linear convolution between the given signal $x(n)$ and $\hat{c}^{(2)}_{q,k}(n-m)$ is an approximation to the second-order derivative of $x(n)$.*

From the above theorem, we state that, an LTI system with CCPS$^{(2)}$ as an impulse response requires different constraints on CCPS$^{(2)}$ to approximate the second-order derivative compared to a system employing CCPS$^{(1)}$ or RS as its impulse response. Additionally, from the definitions of CCPSs, we can say that CCPS$^{(1)}$ and CCPS$^{(2)}$ are HT pairs, i.e., HT of CCPS$^{(1)}$ is equal to CCPS$^{(2)}$ and vice-versa. Given the derivative properties of CCPS$^{(1)}$, it is crucial to derive the derivative properties of CCPS$^{(2)}$ for a comprehensive understanding of the analytical signal, which conveys both amplitude and phase information. This understanding is essential for various applications, including envelope detection [20] and phase tracking [12].

3.2 Applications

3.2.1 Image Edge Detection

Derivative property is an essential tool in signal processing, enabling a wide range of applications such as feature extraction, system analysis, filtering, etc [20, 9, 7]. Here, we address the fundamental image edge detection problem

using CCPS$^{(2)}$ as a first-order derivative. The primary reason for selecting the image edge detection problem as an application stems from our approach to proving the first-order derivative approximation of an LTI system. Specifically, we utilized three distinct properties (refer to Section 2.1) to prove that an LTI system with CCPS$^{(2)}$ as its impulse response can effectively approximate the first-order derivative. This approach is well-established in the literature on image processing [43, 10, 9]. Consequently, we chose to focus on the image edge detection problem.

As stated earlier, image edge detection is a fundamental problem in image processing that involves identifying significant transitions in intensity values within an image. These transitions, or edges, typically correspond to boundaries between different regions, objects, or features in the image, making edge detection crucial for image segmentation and object recognition [10, 9]. Additionally, edge detection plays a vital role in numerous applications, including medical imaging, autonomous driving, and image retrieval systems [10, 9].

For the analysis, we consider the standard Lena image, $\mathbf{x}$, of size 128×128, as depicted in Figure 2 (a). We perform the linear convolution between $\mathbf{x}$ and CCPS$^{(2)}$ in the vertical direction, that is, processing one column of $\mathbf{x}$ at a time. The results are then compared to those obtained using RS and CCPS$^{(1)}$. Consider $q = 5$, then there are $\frac{\varphi(q)}{2} = 2$ possible k values in (1), resulting in two distinct CCPSs$^{(2)}$, denoted as $\hat{c}^{(2)}_{5,1}(n)$ and $\hat{c}^{(2)}_{5,2}(n)$. Figure 2 (b) and (c) depict the results of convolving $\mathbf{x}$ with $\hat{c}^{(2)}_{5,1}(n)$ and $\hat{c}^{(2)}_{5,2}(n)$, respectively, in the vertical direction. From these figures, we can observe that CCPS$^{(2)}$ effectively detects edges in the image by acting as a derivative operator. Additionally, each $\hat{c}^{(2)}_{q,k}(n)$ possesses a unique frequency of $\frac{2\pi k}{q}$ or $\frac{2\pi(q-k)}{q}$ [27], resulting in the frequency spectrum of the convolution output being concentrated around these values.

Comparison with RS: In contrast to CCPS$^{(2)}$, there is only one RS for a given $q > 2$, generated by adding $\varphi(q)$ CESs having a period exactly equal to q, where the unique frequency of each CES is $\frac{2\pi k}{q}$, $(q, k) = 1$ [40]. Figure 2 (d) depicts the convolution result of $\mathbf{x}$ with $\hat{c}_5(n)$ in the vertical direction. Note that RS is also able to extract the image edge information. However, since RS has multiple discrete frequencies, a fine edge detection in an image can be achieved using $\hat{c}^{(2)}_{q,k}(n)$ over $\hat{c}_q(n)$. This improved precision in edge detection can be validated from Figure 2 (b)-(d).

Comparison with CCPS$^{(1)}$: Similar to CCPS$^{(2)}$, for $q = 5$, there are $\frac{\varphi(q)}{2} = 2$ distinct CCPSs$^{(1)}$, denoted as $\hat{c}^{(2)}_{5,1}(n)$ and $\hat{c}^{(2)}_{5,2}(n)$. Figure 2 (e) and (f) depict the results of convolving $\mathbf{x}$ with $\hat{c}^{(1)}_{5,1}(n)$ and $\hat{c}^{(2)}_{5,2}(n)$, respectively, in the vertical direction. Observe that CCPS$^{(1)}$ is also able to detect the edge information effectively. Since CCPS$^{(1)}$ and CCPS$^{(2)}$ are HT pairs, both $x(n) * \hat{c}^{(1)}_{q,k}(n)$ and $x(n) * \hat{c}^{(2)}_{q,k}(n)$ convey the same frequency information with

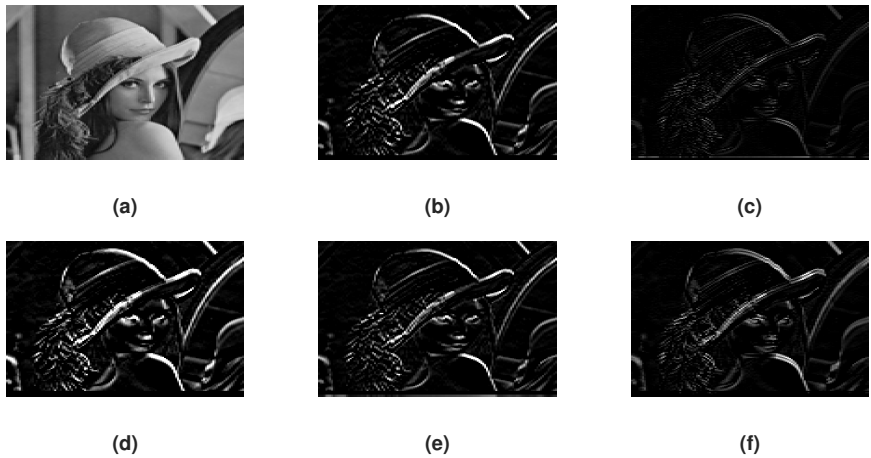

Figure 2: (a) Lena image. Convolving Lena's image in the vertical direction: (b)-(c) With $\hat{c}^{(2)}_{5,1}(n)$ and $\hat{c}^{(2)}_{5,2}(n)$; (d) With $\hat{c}_5(n)$; (e)-(f) With $\hat{c}^{(1)}_{5,1}(n)$ and $\hat{c}^{(1)}_{5,2}(n)$.

a difference in the phase information. Here, the computation of $x(n) * \hat{c}^{(1)}_{q,k}(n)$ and $x(n) * \hat{c}^{(2)}_{q,k}(n)$ involves real-valued operations, whereas the computation of $x(n) * \hat{c}_q(n)$ involves integer-valued operations. Thus, extracting the edge information using CCPSs requires a higher computational complexity than using RS.

3.2.2 ECG Preprocessing

In this section, we present another application to demonstrate the use of CCPS$^{(2)}$ as a derivative operator. R-peak (QRS complex) delineation is a critical step in ECG signal analysis, with various applications [17, 2, 15, 33, 34]. However, directly estimating R-peak information from raw ECG signals is challenging. Therefore, it is common practice to preprocess ECG signals to enhance R-peak delineation. The QRS complex in a typical ECG signal exhibits sudden changes, which can be effectively captured using a derivative operator. Here, we use CCPS$^{(2)}$ for this purpose, and later compare its performance with CCPS$^{(1)}$ and RS.

For our analysis, we use a 10-second ECG recording sampled at 500 Hz from record number 19 of person 1 in the ECG-ID database [8]. To simplify the computation, we down-sampled the data by a factor of 8, resulting in a 625-sample signal with a sampling frequency of 62.5 Hz, as shown in Figure 3 (a). The raw ECG signal contains a significant T-wave (following the QRS

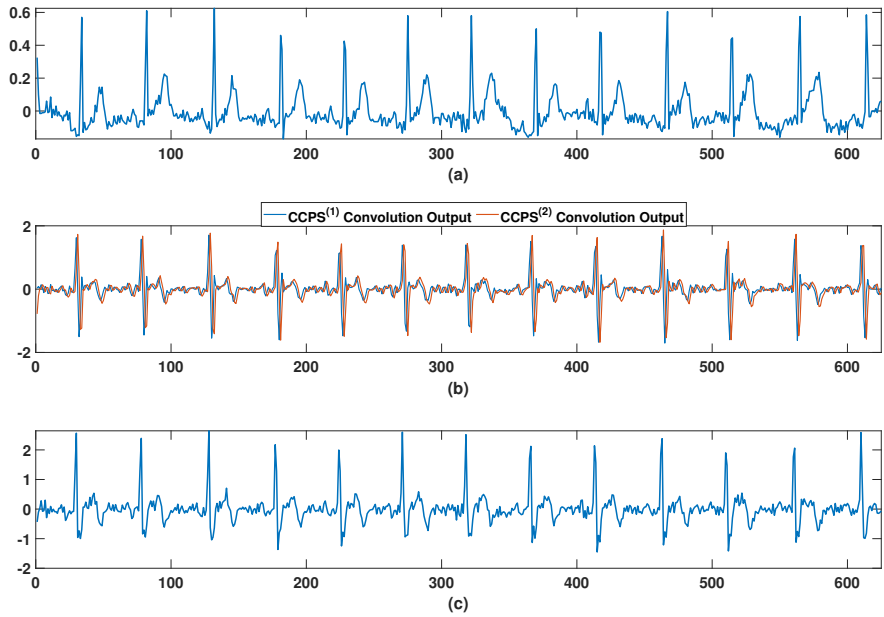

Figure 3: (a) Original ECG signal. Convolving ECG signal: (b) With $\hat{c}_{5,1}^{(1)}(n)$ and $\hat{c}_{5,1}^{(2)}(n)$; (c) With $\hat{c}_5(n)$.

complex), making direct R-peak estimation less accurate. Therefore, before feeding it into an algorithm, we first preprocess the ECG signal using CCPS$^{(2)}$. Specifically, we perform the convolution operation between the ECG signal and $\hat{c}_{5,1}^{(2)}(n)$. The result of this convolution, depicted in Figure 3 (b), shows that the R-peak information is amplified, while the T-wave is attenuated, allowing for improved R-peak estimation using standard methods such as adaptive thresholding [17]. The choice of $\hat{c}_{5,1}^{(2)}(n)$ is based on the frequency range of the QRS complex, typically 8–20 Hz [6]. With a sampling frequency of 62.5 Hz, the discrete frequency associated with $\hat{c}_{5,1}^{(2)}(n)$ is 12.5 Hz. Hence, the spectrum of the convolved signal is concentrated around 12.5 Hz, which falls within the QRS complex frequency range.

Comparison with CCPS$^{(1)}$: Figure 3 (b) also shows the convolution output between ECG signal and $\hat{c}_{5,1}^{(1)}(n)$. Since CCPS$^{(1)}$ and CCPS$^{(2)}$ form an HT pair, they contain the same frequency information with a phase shift. This is evident in the Figure 3 (b).

Comparison with RS: Figure 3 (c) shows the convolution output using $\hat{c}_5(n)$. While RS also amplifies the R-peak information, it retains significant

T-wave content. The reason is that an RS has multiple frequencies associated with it. For instance, in this example, $\hat{c}_5(n)$ is generated by adding CESs with frequencies 12.5 Hz and 25 Hz. As a result, one can observe significant T-wave information in Figure 3 (c).

4 Non-Overlapping DFT Coefficients

In this section, we show that the DFT coefficients of any two distinct CCPS$^{(1)}$, CCPS$^{(2)}$, or CCPS$^{(1)}$ and CCPS$^{(2)}$ do not overlap. Specifically, we have the following theorem.

Theorem 4. *The q-point DFT coefficients of any two q-length sequences $c^{(1)}_{q_1,k_1}(n-l_1)$ and $c^{(2)}_{q_2,k_2}(n-l_2)$ never overlap, where $q_1 \neq q_2$ and $q = lcm(q_1, q_2)$.*

Proof. For a given $q_2 \in \mathbb{N}$ and $k_2 \in \hat{U}_{q_2}$, the q_2-point DFT of $c^{(2)}_{q_2,k_2}(n)$, $C^{(2)}_{q_2,k_2}(K)$, equal to [27]

$$C^{(2)}_{q_2,k_2}(K) = \begin{cases} -jq_2, & \text{if } K = k_2 \\ jq_2, & \text{if } K = q_2 - k_2 \\ 0, & \text{otherwise} \end{cases}.$$

Here $c^{(2)}_{q_2,k_2}(n)$ can be rewritten as $c^{(2)}_{q,k_2m_2}(n)$, where $q = m_2q_2$, $m_2 \in \mathbb{Z}$. The q-point DFT of $c^{(2)}_{q,k_2m_2}(n-l_2)$, $C^{(2)}_{q,k_2m_2,l_2}(K)$, is

$$C^{(2)}_{q,k_2m_2,l_2}(K) = \begin{cases} -jqe^{\frac{-j2\pi k_2 l_2}{q_2}}, & \text{if } K = k_2m_2 \\ jqe^{\frac{j2\pi k_2 l_2}{q_2}}, & \text{if } K = q - k_2m_2 \\ 0, & \text{otherwise} \end{cases}.$$

Similarly, if we compute the q-point DFT of $c^{(1)}_{q,k_1m_1}(n-l_1)$, where $q = m_1q_1$ and $m_1 \in \mathbb{Z}$, we get the non-zero coefficient values at $K = k_1m_1$ and $K = q - k_1m_1$. The DFT coefficients of both these sequences will overlap if $k_1m_1 = k_2m_2$ or $k_1m_1 = q - k_2m_2$, implying $k_1q_2 = k_2q_1$ or $k_1q_2 = q_1(q_2 - k_2)$; this equality is valid if and only if $q_1 = q_2$, since $(k_1, q_1) = 1$ and $(k_2, q_2) = (q_2 - k_2, q_2) = 1$. This contradicts our assumption of $q_1 \neq q_2$. □

Likewise, by using the same procedure as in the proof of the previous theorem, we can demonstrate the following theorem:

Theorem 5. *The q-point DFT coefficients of any two sequences $c^{(1)}_{q_1,k_1}(n-l_1)$ and $c^{(1)}_{q_2,k_2}(n-l_2)$, or $c^{(2)}_{q_1,k_1}(n-l_1)$ and $c^{(2)}_{q_2,k_2}(n-l_2)$ never overlap, where $q = lcm(q_1, q_2)$ and $q_1 \neq q_2$.*

Figure 4 (a)-(d) depict the magnitude spectra of the 24-point DFT coefficients of $c_{8,3}^{(1)}(n-1)$, $c_{8,3}^{(2)}(n-1)$, $c_{6,1}^{(1)}(n-2)$, and $c_{6,1}^{(2)}(n-2)$, respectively. One can verify Theorem 4 and Theorem 5 from this example as well. Note that the DFT coefficients of any two sequences are non-overlap, implying that both sequences are orthogonal to each other. Hence, we can state that any two CCPSs are orthogonal to each other. This property plays an important role in signal representation.

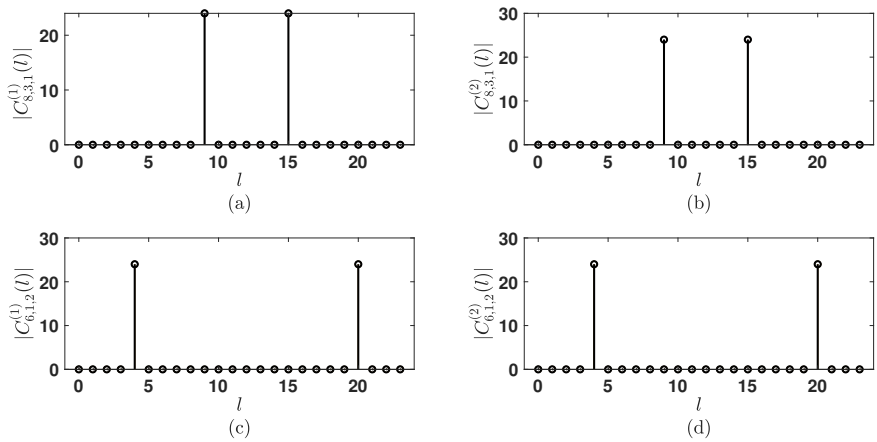

Figure 4: (a)-(d) Magnitude spectrum of 24-point DFT coefficients of $c_{8,3}^{(1)}(n-1)$, $c_{8,3}^{(2)}(n-1)$, $c_{6,1}^{(1)}(n-2)$, and $c_{6,1}^{(2)}(n-2)$, respectively.

4.1 Application

The property of non-overlapping DFT coefficients is crucial in modulation techniques within wireless communication because it ensures that different data symbols are orthogonally modulated, which is key to minimizing interference and maximizing spectral efficiency [42, 22, 35]. Literature has established that CESs and RSs also satisfy this non-overlapping DFT coefficients property [16], [40]. Consequently, these summations serve as the foundation for the Ramanujan subspace (orthogonal periodic subspace) [16, 27, 40]. Ramanujan subspaces are instrumental in representing finite-length signals. Using CESs, RSs, and CCPSs (both CCPS$^{(1)}$ & CCPS$^{(2)}$ together) as a basis for the Ramanujan subspace leads to DFT [3], RPT [40], and OCCPT [27], respectively. In the literature, DFT and RPT are employed in modulation/demodulation schemes such as Orthogonal Frequency Division Multiplexing (OFDM) [3, 1] and Ramanujan Periodic Subspace Division Multiplexing (RPSDM) [35], respectively.

Analogously, using OCCPT signal representation (whose mathematical closed-form equations are given in [27]) introduces a new modulation/demodulation scheme: Orthogonal Complex Conjugate Periodic Subspace Division Multiplexing (OCCPSDM). While a comprehensive mathematical analysis of OCCPSDM is beyond the scope of this paper, we provide an initial comparison of its Peak-to-Average Power Ratio (PAPR) performance and computational complexity relative to the aforementioned schemes. The commonality among the transformation matrices of DFT, RPT, and OCCPT is that they all belong to the Nested Periodic Matrix (NPM) family [39]. In addition to DFT, RPT, and OCCPT, Natural Basis Matrices (NBMs) and Random Periodic Matrices (RPMs) are also members of the NPM family, which has been used to estimate periodic information from signals [37, 39]. Furthermore, any transformation matrix belonging to the NPM family is a full-rank matrix. Therefore, in this work, we generate modulation symbols using both NBMs and RPMs, and compare their PAPR with that of the proposed OCCPSDM. We refer to the modulation and demodulation schemes based on NBM and RPM as Natural Basis Periodic Subspace Division Multiplexing (NBPSDM) and Random Gaussian Periodic Subspace Division Multiplexing (RGPSDM), respectively. To the best of our knowledge, this is the first study to utilize both NBM and RPM for modulation and demodulation. The mathematical analysis of both NBPSDM and RGPSDM remains an open problem to be explored. It is important to note that while both NBM and RPM are full-rank matrices, they are not orthogonal [39], hence, the receiver computational complexity is high in both NBPSDM and RGPSDM. Furthermore, there are no fast algorithms for computing signal representation coefficients based on NBM and RPM. However, NBM is a sparse matrix, specifically, an $L \times L$ matrix, where $L = 2^n,\ n \in \mathbb{N}$, has $L + \frac{L}{2} log_2(L)$ non-zero elements. Therefore, we exploit the sparsity of NBM to compute NBM-based representation coefficients efficiently, while for RPM-based representations, we use a direct method via matrix multiplication.

Figure 5 shows the Complementary Cumulative Distribution Function (CCDF) of PAPR [4] for OFDM, RPSDM, OCCPSDM, NBPSDM, and RGPSDM for $N = 128,\ 256$, and 512, where N denotes the number of sub-carriers. It is evident from Figure 5 that the PAPR of OCCPSDM approximates OFDM and is slightly better than NBPSDM. Whereas, the PAPR of RPSDM and RGPSDM is lesser; specifically, RPSDM maintains around $2dB$ difference for CCDFs less than 0.1 [35].

For a given complex sequence of length L, where $L = 2^m$ and $m \in \mathbb{N}$, Table 1 presents the number of real multiplications required for computing OCCPT (using FOCCPT [27]), DFT (using FFT), RPT (exploiting the sparse nature of the transform matrix [35]), NBM-based representation (using sparse nature of the transform matrix), and RPM-based representation (using direct method). From Table 1, it is evident that for larger values of L, OCCPSDM

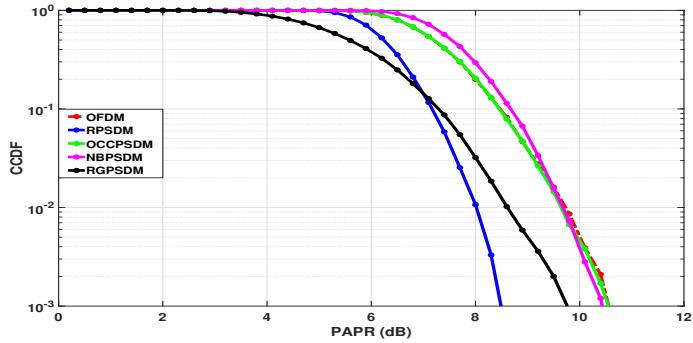

(a) For $N = 128$.

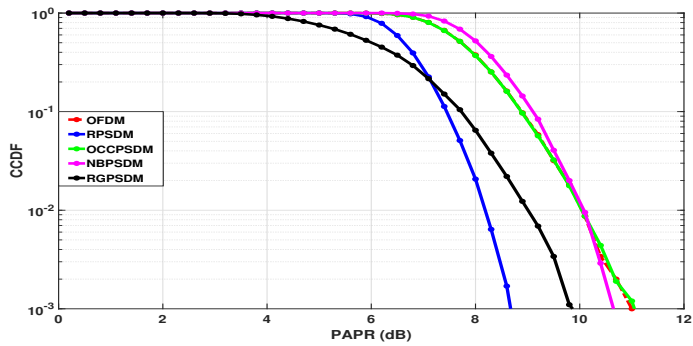

(b) For $N = 256$.

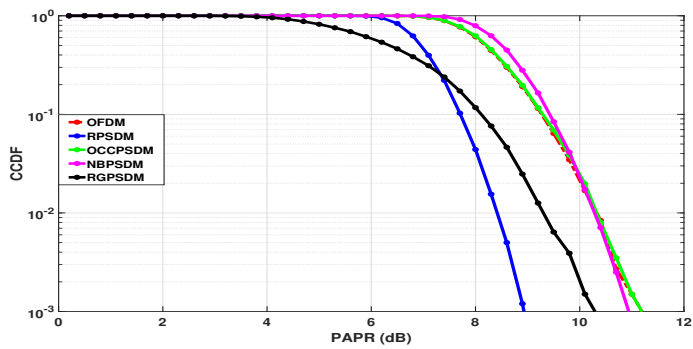

(c) For $N = 512$.

Figure 5: (a)-(c) PAPR comparison of various modulation techniques.

Table 1: Comparison of computational complexity between different modulation/demodulation schemes.

Number of Real Multiplications			
Modulation/Demodulation	L =128	L = 256	L = 512
OFDM ($2Llog_2(L)$)	1792	4096	9216
RPSDM ($2Llog_2(L) + 2L$)	2048	4608	10240
OCCPSDM ($2Llog_2(L) - 2L + 2$)	1538	3586	8194
NBPSDM ($Llog_2(L) + 2L$)	1152	2560	5632
RGPSDM ($2L^2$)	32768	131072	524288

and NBPSDM exhibit a significant computational complexity advantage over the other methods. However, it is important to note that the OCCPSDM transformation matrix is orthogonal, whereas NBPSDM is non-orthogonal. This non-orthogonality increases computational complexity at the receiver end for NBPSDM. Consequently, OCCPSDM emerges as a promising candidate for applications in 5G systems employing OFDM. While this paper highlights the importance of non-overlapping DFT coefficients of both CCPS$^{(1)}$ and CCPS$^{(2)}$ through a modulation/demodulation scheme, a detailed computational analysis of OCCPSDM, NBPSDM, and RGPSDM remains a subject for future investigation. In addition to its role in communication, the property of non-overlapping DFT coefficients has numerous applications in digital signal processing. This includes audio and image processing, where non-overlapping DFT coefficients are leveraged to develop efficient algorithms for tasks such as filtering, compression, and enhancement [16, 20, 14].

A detailed comparison of the properties of CCPS$^{(1)}$ and CCPS$^{(2)}$, derived in this work and in [31, 26, 27], is provided in Table 2.

5 Conclusion

In this study, we addressed the gap in the literature concerning Complex Conjugate Pair Sum of type-2 (CCPS$^{(2)}$) by building upon established concepts such as Ramanujan Sum (RS), Complex Exponential Sequences (CESs), and CCPS$^{(1)}$. We demonstrated that CCPS$^{(2)}$ can effectively approximate both first- and second-order derivatives in Linear Time-Invariant (LTI) systems, with practical applications in image edge detection and ECG signal preprocessing. Through these applications, we showed that CCPS$^{(2)}$ and CCPS$^{(1)}$ extract the same frequency information with a phase shift, confirming that they form a Hilbert transform pair. In comparison to RS, we demonstrated that both CCPS$^{(1)}$ and CCPS$^{(2)}$ achieve finer feature extraction. Additionally, we established that the DFT coefficients of CCPS$^{(1)}$ and CCPS$^{(2)}$ do not

Table 2: Properties of $\text{CCPS}^{(1)}$ and $\text{CCPS}^{(2)}$.

Property Name	**$\text{CCPS}^{(1)}$**	**$\text{CCPS}^{(2)}$**
Definition	$c_{q,k}^{(1)}(n) = 2Mcos\left(\frac{2\pi kn}{q}\right)$, $k \in \hat{U}_q$, $n \in \mathbb{Z}$, $q \in \mathbb{N}$, $M = \begin{cases} \frac{1}{2}, & \text{if } q = 1 \text{ or } 2 \\ 1, & \text{if } q > 2 \end{cases}$	$c_{q,k}^{(2)}(n) = \begin{cases} 1, & \text{if } q = 1 \\ (-1)^n, & \text{if } q = 2,\ k \in \hat{U}_q, \\ 2sin\left(\frac{2\pi kn}{q}\right), & \text{if } q > 2 \end{cases}$ $n \in \mathbb{Z}$, $q \in \mathbb{N}$
Sequence Type	Real-valued	Real-valued
Periodicity	$c_{q,k}^{(1)}(n+q) = c_{q,k}^{(1)}(n)$	$c_{q,k}^{(2)}(n+q) = c_{q,k}^{(2)}(n)$
Symmetry	$c_{q,k}^{(1)}(q-n) = c_{q,k}^{(1)}(n)$	$c_{q,k}^{(2)}(q-n) = -c_{q,k}^{(2)}(n)$, if $q > 2$
Sum	$\sum_{n=0}^{q-1} c_{q,k}^{(1)}(n) = 0$	$\sum_{n=0}^{q-1} c_{q,k}^{(2)}(n) = 0$
Sum-of-Squares	$\sum_{n=0}^{q-1} \left(c_{q,k}^{(1)}(n)\right)^2 = 2qM$	$\sum_{n=0}^{q-1} \left(c_{q,k}^{(2)}(n)\right)^2 = 2qM$
Sequence's First Element	$c_{q,k}^{(1)}(0) = 2,\ \forall\ q > 2$	$c_{q,k}^{(2)}(0) = 0,\ \forall\ q > 2$
DFT Coefficients	$C_{q,k}^{(1)}(K) = \begin{cases} q, & \text{if } K = k \text{ (or) } q-k \\ 0, & \text{otherwise} \end{cases}$	$C_{q,k}^{(2)}(K) = \begin{cases} -jq, & \text{if } K = k \\ jq, & \text{if } K = q-k \\ 0, & \text{otherwise} \end{cases}$
Orthogonality	$\sum_{n=0}^{q-1} c_{q_1,k_1}^{(1)}(n-l_1)c_{q_2,k_2}^{(1)}(n-l_2) = 2qMcos\left(\frac{2\pi k_1(l_1-l_2)}{q_1}\right)\delta(q_1 - q_2)\delta(k_1-k_2)$, $q = lcm(q_1,q_2)$	$\sum_{n=0}^{q-1} c_{q_1,k_1}^{(2)}(n-l_1)c_{q_2,k_2}^{(2)}(n-l_2) = 2qMcos\left(\frac{2\pi k_1(l_1-l_2)}{q_1}\right)\delta(q_1 - q_2)\delta(k_1-k_2)$, $q = lcm(q_1,q_2)$
Non-Overlapping DFT Coefficients	The $q = lcm(q_1,q_2)$-point DFT coefficients of $c_{q_1,k_1}^{(1)}(n)$ and $c_{q_2,k_2}^{(1)}(n)$ never overlap, where $q_1 \neq q_2$	The $q = lcm(q_1,q_2)$-point DFT coefficients of $c_{q_1,k_1}^{(2)}(n)$ and $c_{q_2,k_2}^{(2)}(n)$ never overlap, where $q_1 \neq q_2$
	The $q = lcm(q_1,q_2)$-point DFT coefficients of $c_{q_1,k_1}^{(1)}(n)$ and $c_{q_2,k_2}^{(2)}(n)$ never overlap, where $q_1 \neq q_2$	
First-Order Derivative	Yes	Yes
Second-Order Derivative	If $q = 2b+1$ and $m = b$, where $b \in \mathbb{N}$, then $x(n) * \hat{c}_{q,k}^{(1)}(n-m)$ is an approximation to the second-order derivative of $x(n)$	If $q = 4b+2$ and $m \in \{b, 3b+1\}$, where $b \in \mathbb{N}$, then $x(n) * \hat{c}_{q,k}^{(2)}(n-m)$ is an approximation to the second-order derivative of $x(n)$

overlap, supporting their use in the newly introduced Orthogonal Complex Conjugate Periodic Subspace Division Multiplexing (OCCPSDM). This modulation scheme offers a comparable Peak-to-Average Power Ratio (PAPR) with reduced computational complexity relative to other existing modulation schemes.

References

[1] N. Ali, R. Almahainy, A. Al-Shabili, N. Almoosa, and R. Abd-Alhameed, "Analysis of improved μ-law companding technique for OFDM systems", *IEEE Transactions on Consumer Electronics*, 63(2), 2017, 126–34, DOI: 10.1109/TCE.2017.014753.

[2] L. Biel, O. Pettersson, L. Philipson, and P. Wide, "ECG analysis: a new approach in human identification", *IEEE Transactions on Instrumentation and Measurement*, 50(3), 2001, 808–12, DOI: 10.1109/19.930458.

[3] J. A. C. Bingham, "Multicarrier modulation for data transmission: an idea whose time has come", *IEEE Communications Magazine*, 28(5), 1990, 5–14.

[4] Y. S. Cho, J. Kim, W. Y. Yang, and C. G. Kang, *MIMO-OFDM wireless communications with MATLAB*, John Wiley & Sons, 2010.

[5] S. w. Deng and J. q. Han, "Signal Periodic Decomposition With Conjugate Subspaces", *IEEE Trans. Signal Process.*, 64(22), November 2016, 5981–92, ISSN: 1053-587X, DOI: 10.1109/TSP.2016.2600509.

[6] M. Elgendi, M. Jonkman, and F. De Boer, "Frequency bands effects on QRS detection", English, in, Vol. 1, Institute for Systems, Technologies of Information, Control, and Communication (INSTICC), 2010, 428–31, ISBN: 978-989-674-018-4.

[7] G. F. Franklin, J. D. Powell, A. Emami-Naeini, *et al.*, *Feedback control of dynamic systems*, Vol. 3, Addison-Wesley Reading, MA, 1994.

[8] A. L. Goldberger, L. A. N. Amaral, L. Glass, J. M. Hausdorff, P. C. Ivanov, and R. G. Mark et al., "PhysioBank, PhysioToolkit, and PhysioNet: components of a new research resource for complex physiologic signals", *Circulation*, 101(23), 2000, e215–e220.

[9] R. C. Gonzalez, *Digital image processing*, Pearson education india, 2009.

[10] A. K. Jain, *Fundamentals of digital image processing*, Englewood Cliffs, NJ, USA:Prentice-Hall, 1989.

[11] H. Liao and L. Su, "Monaural Source Separation Using Ramanujan Subspace Dictionaries", *IEEE Signal Processing Letters*, 25(8), August 2018, 1156–60, ISSN: 1070-9908, DOI: 10.1109/LSP.2018.2847236.

[12] S. L. Marple Jr, *Digital spectral analysis*, Courier Dover Publications, 2019.

[13] P. Mathur, V. K. Chakka, and S. B. Shah, "Ramanujan Periodic Subspace Based Epileptic EEG Signals Classification", *IEEE Sensors Lett.*, 5(7), 2021, 1–4, DOI: 10.1109/LSENS.2021.3086755.

[14] S. K. Mitra, *Digital signal processing: a computer-based approach*, McGraw-Hill Higher Education, 2001.

[15] G. V. S. S. K. R. Naganjaneyulu, B. S. Shaik, and A. Narasimhadhan, "R peak delineation in ECG signal based on polynomial chirplet transform using adaptive threshold", in *11th International Conference on Industrial and Information Systems (ICIIS)*, 2016, 856–60, DOI: 10.1109/ICIINFS.2016.8263058.

[16] A. V. Oppenheim and R. W. Schafer, *Discrete-time Signal Processing*, 3rd, Upper Saddle River, NJ, USA: Prentice Hall, 2009, ISBN: 0131988425, 9780131988422.

[17] J. Pan and W. J. Tompkins, "A Real-Time QRS Detection Algorithm", *IEEE Transactions on Biomedical Engineering*, BME-32(3), 1985, 230–6, DOI: 10.1109/TBME.1985.325532.

[18] S. C. Pei and K. W. Chang, "Odd Ramanujan Sums of Complex Roots of Unity", *IEEE Signal Processing Letters*, 14(1), January 2007, 20–3, ISSN: 1070-9908, DOI: 10.1109/LSP.2006.881527.

[19] M. Planat, "Ramanujan sums for signal processing of low frequency noise", in *Frequency Control Symposium and PDA Exhibition, 2002. IEEE International*, 2002, 715–20, DOI: 10.1109/FREQ.2002.1075974.

[20] J. G. Proakis, *Digital signal processing: principles, algorithms, and applications, 4/E*, Pearson Education India, 2007.

[21] S. Ramanujan, "On certain trigonometrical sums and their applications in the theory of numbers", *Trans. Cambridge Philos. Soc.*, 22(13), 1918, 259–76.

[22] T. S. Rappaport, *Wireless communications: principles and practice*, Cambridge University Press, 2024.

[23] P. Saidi, G. Atia, and A. Vosoughi, "Detection of Visual Evoked Potentials using Ramanujan Periodicity Transform for real time brain computer interfaces", in *2017 IEEE International Conference on Acoustics, Speech and Signal Processing (ICASSP)*, March 2017, 959–63, DOI: 10.1109/ICASSP.2017.7952298.

[24] P. Saidi, G. Atia, and A. Vosoughi, "On robust detection of brain stimuli with Ramanujan Periodicity Transforms", in *2017 51st Asilomar Conference on Signals, Systems, and Computers*, October 2017, 729–33, DOI: 10.1109/ACSSC.2017.8335440.

[25] S. Samadi, M. O. Ahmad, and M. N. S. Swamy, "Ramanujan Sums and Discrete Fourier Transforms", *IEEE Signal Processing Letters*, 12(4), April 2005, 293–6, ISSN: 1070-9908, DOI: 10.1109/LSP.2005.843775.

[26] S. B. Shah, V. K. Chakka, and A. S. Reddy, "On Complex Conjugate Pair Sums and Complex Conjugate Subspaces", *IEEE Signal Process. Lett.*, 26(9), September 2019, 1403–7, DOI: 10.1109/LSP.2019.2932717.

[27] S. B. Shah, V. K. Chakka, and A. S. Reddy, "Orthogonal and Non-Orthogonal Signal Representations Using New Transformation Matrices Having NPM Structure", *IEEE Trans. Signal Process.*, 68, 2020, 1229–42, ISSN: 1941-0476, DOI: 10.1109/TSP.2020.2971936.

[28] S. B. Shah and V. K. Chakka, "Signal Representation Using Ramanujan Subspaces Utilizing A Prior Signal Information", in *2020 International Conference on Signal Processing and Communications (SPCOM)*, 2020, 1–5, DOI: 10.1109/SPCOM50965.2020.9179618.

[29] B. Shah Shaik, V. K. Chakka, S. Goli, and A. S. Reddy, "Removal of narrowband interference (PLI in ECG signal) using Ramanujan periodic transform (RPT)", in *2016 International Conference on Signal Processing and Communication (ICSC)*, December 2016, 233–7, DOI: 10.1109/ICSPCom.2016.7980582.

[30] B. S. Shaik, V. K. Chakka, and S. Goli, "Ramanujan and DFT mixed basis representation for removal of PLI in ECG signal", in *2017 4th International Conference on Signal Processing and Integrated Networks (SPIN)*, February 2017, 509–12, DOI: 10.1109/SPIN.2017.8050003.

[31] B. S. Shaik, V. K. Chakka, and A. S. Reddy, "A new signal representation using complex conjugate pair sums", *IEEE Signal Process. Lett.*, 26(2), February 2019, 252–6, ISSN: 1070-9908, DOI: 10.1109/LSP.2018.2887025.

[32] B. S. Shaik and V. K. Chakka, "Joint reduction of baseline wander, PLI and its harmonics in ECG signal using Ramanujan Periodic Transform", in *2016 IEEE Annual India Conference (INDICON)*, 2016, 1–5, DOI: 10.1109/INDICON.2016.7838897.

[33] B. S. Shaik, G. V. S. S. K. R. Naganjaneyulu, and A. Narasimhadhan, "A novel approach for QRS delineation in ECG signal based on chirplet transform", in *IEEE International Conference on Electronics, Computing and Communication Technologies (CONECCT)*, 2015, 1–5, DOI: 10.1109/CONECCT.2015.7383914.

[34] B. S. Shaik, G. Naganjaneyulu, T. Chandrasheker, and A. Narasimhadhan, "A Method for QRS Delineation Based on STFT Using Adaptive Threshold", *Procedia Computer Science*, 54, 2015, 646–53, ISSN: 1877-0509, DOI: https://doi.org/10.1016/j.procs.2015.06.075, https://www.sciencedirect.com/science/article/pii/S187705091501399X.

[35] G. Srikanth, V. K. Chakka, and S. B. Shah, "Ramanujan periodic subspace division multiplexing", *IET Commun.*, 13(15), 2019, 2296–303, DOI: 10.1049/iet-com.2018.5828.

[36] L. Sugavaneswaran, S. Xie, K. Umapathy, and S. Krishnan, "Time-Frequency Analysis via Ramanujan Sums", *IEEE Signal Processing Letters*, 19(6), June 2012, 352–5, ISSN: 1070-9908, DOI: 10.1109/LSP.2012.2194142.

[37] S. Tenneti and P. P. Vaidyanathan, "Dictionary Approaches For Identifying Periodicities in Data", in *2014 48th Asilomar Conference on Signals, Systems and Computers*, November 2014, 1967–71, DOI: 10.1109/ACSSC.2014.7094814.

[38] S. V. Tenneti and P. P. Vaidyanathan, "Detecting tandem repeats in DNA using Ramanujan Filter Bank", in *2016 IEEE International Symposium on Circuits and Systems (ISCAS)*, May 2016, 21–4, DOI: 10.1109/ISCAS.2016.7527160.

[39] S. V. Tenneti and P. P. Vaidyanathan, "Nested Periodic Matrices and Dictionaries: New Signal Representations for Period Estimation", *IEEE Transactions on Signal Processing*, 63(14), July 2015, 3736–50, ISSN: 1053-587X, DOI: 10.1109/TSP.2015.2434318.

[40] P. P. Vaidyanathan, "Ramanujan sums in the context of signal processing-Part I: Fundamentals", *IEEE Trans. Signal Process.*, 62(16), August 2014, 4145–57, ISSN: 1053-587X, DOI: 10.1109/TSP.2014.2331617.

[41] P. P. Vaidyanathan, "Ramanujan sums in the context of signal processing-Part II: FIR representations and applications", *IEEE Trans. Signal Process.*, 62(16), August 2014, 4158–72, ISSN: 1053-587X, DOI: 10.1109/TSP.2014.2331624.

[42] S. Weinstein and P. Ebert, "Data Transmission by Frequency-Division Multiplexing Using the Discrete Fourier Transform", *IEEE Transactions on Communication Technology*, 19(5), 1971, 628–34, DOI: 10.1109/TCOM.1971.1090705.

[43] D. K. Yadav, G. Kuldeep, and S. D. Joshi, "Ramanujan Sums as Derivatives and Applications", *IEEE Signal Process.Lett.*, 25(3), March 2018, 413–6, ISSN: 1070-9908, DOI: 10.1109/LSP.2017.2721966.